JPET Fast Forward. Published on September 27, 2005 as DOI: 10.1124/jpet.105.092312

JPET #92312

Title Page

Targeted antioxidative and neuroprotective properties of the dopamine agonist Pramipexole and its non-dopaminergic enantiomer SND919CL2x.

R. Danzeisen, B. Schwalenstoecker, F.Gillardon, E. Buerger, V. Krzykalla, K. Klinder, L. Schild, B. Hengerer, A.C. Ludolph, C. Dorner-Ciossek and L. Kussmaul

RD, BS, ACL: Department of Neurology, Albert-Einstein-Allee 11 (O25), University of Ulm, Ulm, Germany

FG, EB, BH, CDC, LK: Department of CNS Research, Boehringer-Ingelheim Pharma GmbH &Co. KG, Biberach, Germany

VK: Department of Medical Data Services, Boehringer-Ingelheim Pharma GmbH &Co. KG, Biberach, Germany

KK: Department of Drug Discovery Support, Boehringer-Ingelheim Pharma GmbH &Co. KG, Biberach, Germany

LS: Institute of Clinical Chemistry and Pathological Biochemistry, Department of Pathological Biochemistry, Otto-von-Guericke-University, Magdeburg, Germany.

Running Title Page

Running Title: Targeted antioxidative neuroprotection by Pramipexole

Corresponding author
Lothar Kussmaul
Department of CNS Research
Boehringer-Ingelheim Pharma GmbH &Co. KG
Birkendorfer Straße 65
88397 Biberach an der Riss
Phone: +49(0)7351-54-8668 or 0044-1223252812
Fax +49(0)7351-54-2171
e-mail: lothar.kussmaul@bc.boehringer-ingelheim.com

Number of text pages: **43**
Number of tables: **1**
Number of figures: **6**
Number of references: ***41*** (max. 40)
Number of words in the *Abstract: **247** (max. 250)*
Number of words *Introduction: **735** (max.750)*
Number of words *Discussion: **1600** (max. 1500)*

List of Abbreviations
ALS, Amyotrophic Lateral Sclerosis; BME, Basal modified Eagle medium; DETA, (Z)-1-[2-(2-Aminoethyl)-N-(2-ammonioethyl)amino]diazen-1-ium-1,2-diolate; DAF, 4,5-Diaminofluorescein; DMEM, Dulbecco's Modified Eagle Media; HBSS, Hanks' balanced salt solution; HRP, horseradish peroxidase; ROS, reactive oxygen species

Recommended section assignment: NEUROPHARMACOLOGY

JPET Fast Forward. Published on September 27, 2005 as DOI: 10.1124/jpet.105.092312
This article has not been copyedited and formatted. The final version may differ from this version.

Abstract

Pramipexole has been shown to possess neuroprotective properties *in vitro*, which are partly independent of its dopaminergic agonism. The site of neuroprotective action is still unknown. Using [^{3}H]-Pramipexole we show that the drug enters and accumulates in cells and mitochondria. Detoxification of reactive oxygen species (ROS) by Pramipexole is shown *in vitro* and *in vivo* by evaluating mitochondrial ROS-release and aconitase-2 activity, respectively. Pramipexole and its (+)-enantiomer SND919CL2X (low affinity dopamine agonist) possess equipotent efficacy towards hydrogen peroxide and nitric oxide generated *in vitro*, and inhibit cell death in glutathione-depleted neuroblastoma cells. IC_{50}-values ranged from 15 to 1000 µM, consistent with the reactivity of the respective radical and the compartmentalization of ROS-generation and ROS-detoxification. Finally, both compounds were tested in SOD1-G93A mice, a model of familial Amyotrophic Lateral Sclerosis. SND919CL2X (100 mg/kg) prolongs survival time and preserves motor function, in contrast to Pramipexole (3 mg/kg), which shows an increase in running wheel activity before disease onset, presumably caused by the dopaminergic agonism. We conclude that both enantiomers, in addition to their dopaminergic activity, are able to confer neuroprotective effects by their ability to accumulate in brain, cells and mitochondria where they detoxify ROS. However, a clinical use of Pramipexole as a mitochondria-targeted antioxidant is unlikely, since the high doses needed for antioxidative action *in vitro* are not accessible *in vivo*, due to dopaminergic side effects. In contrast, SND919CL2X may represent the prototype of a mitochondria-targeted neuroprotectant, since it has the same antioxidative properties, without causing adverse effects.

Introduction

Pramipexole (PPX, (-) 2-amino-4,5,6,7-tetrahydro-6-D-propylamino-benzathiazole) is a non-ergot dopamine receptor agonist (subtype: D2 and D3) used for symptomatic treatment of Parkinson's disease. Preclinical studies show that nanomolar concentrations of PPX protect dopaminergic neurons *in vitro* (Ling et al., 1999) or *in vivo (*about 1 mg/kg) (Zou et al., 2000; Anderson et al., 2001; Ramirez et al., 2003) by a receptor-dependent pathway. This is possibly mediated by the high selectivity of PPX for D3- Receptors (Mierau et al., 1995; Ramirez et al., 2003), causing an increase of protective proteins (Ling et al., 1998; Presgraves et al., 2004; Pan et al., 2005).

At higher concentrations (above 10 micromolar), PPX has been shown to be neuroprotective *in vitro* independent of the dopaminergic agonism (Le et al., 2000; Abramova et al., 2002; Gu et al., 2004 and references herein). In addition, SND, the (+) enantiomer of PPX, has been shown to be neuroprotective as well (Abramova et al., 2002; Gu et al., 2004), although its affinity to dopamine receptors is approximately 100-fold less compared to PPX (Mierau, 1995).

Site and mechanism of the receptor-independent action have so far not been shown directly. Several studies described an antioxidative action of the drug and/or a preservation of mitochondrial function, resulting in inhibition of cell death (Cassarino et al., 1998; Kitamura et al., 1998; Kakimura et al., 2001; Abramova et al., 2002; Gu et al., 2004). Since both enantiomers are lipophilic cations it has been hypothesized (Abramova et al., 2002) that they might accumulate in mitochondria, as predicted for

other lipophilic cations (Trapp and Horobin, 2005). However the concept that PPX and/or SND act intracellularly, as mitochondrial targeted antioxidants has not yet been proven.

Mitochondria-targeted antioxidants accumulate in mitochondria and show higher efficacy compared to untargeted antioxidants (Ross et al., 2005). They represent promising candidates to prevent or alleviate mitochondrial oxidative stress which is involved in the pathogenesis of Alzheimer's diseases, Parkinson's disease or amyotrophic lateral sclerosis (ALS) (Andersen, 2004). Due to the lack of an active uptake process, we propose that SND is able to enter neural cells and exert the same properties as PPX. Support for this proposal is given by its equal antioxidative efficacy towards hydrogen peroxide and nitric oxide when compared to PPX, and by equipotent efficacy of SND and PPX to prevent cell death in glutathione-depleted neuroblastoma cells (Maher and Davis, 1996).

This paper addresses those neuroprotective properties of PPX and SND which are not mediated by stimulation of dopamine receptors. Initially, an intracellular site of action is demonstrated by evaluating the uptake properties of [^{3}H]-labeled PPX. We show for the first time that PPX enters neural cells and accumulates in mitochondria driven by mitochondrial membrane potential in a diffusion limited process. In addition, PPX detoxifies ROS within the mitochondria as shown by inhibition of mitochondrial hydrogen peroxide (H_2O_2) release, and by an increase in mitochondrial aconitase activity.

ALS is a devastating disease, progressing from mild motor symptoms to severe paralysis and premature death caused by the degeneration of motor neurons. Twenty percent of familial ALS cases are caused by mutations in superoxide dismutase 1 (SOD1), which expressed in mice result in a phenotype resembling the pathology in patients. Transgenic SOD1 mice represent the predominant model to study ALS pathogenesis and therapy. Neuronal cell death in ALS is at least in part associated with an increase in oxidative stress and mitochondrial alterations (Menzies et al., 2002). Mitochondrial dysfunction seems a likely candidate to explain many facets of ALS, as it is the earliest reported pathologic event in ALS-mice (Bendotti et al., 2001). Mitochondrial pathology may contribute to generate a condition of oxidative stress, and indeed markers of oxidative damage (increased ROS flux, oxidatively modified proteins) have been found in cultured neuronal cells, in transgenic mice and in patients as well (reviewed in Bendotti and Carri, 2004). Furthermore, PPX reduces oxidative stress in ALS patients (Pattee et al., 2003), pointing to the necessity to evaluate PPX and SND for their efficacy in an animal model for ALS.

In order to test for neuroprotection by PPX/SND *in vivo*, transgenic SOD-1 mice were treated with both compounds. Treatment with PPX resulted in pre-onset motor hyperactivity; SND was able to prolong survival and improve motor performance, without causing hyperactivity. This is the first report showing that PPX and SND are able to act as brain- and mitochondrial-targeted antioxidants, which most likely explains the receptor-independent neuroprotective effects observed *in vitro* and *in vivo*.

Methods

Chemicals. All cell culture media and reagents were purchased from Gibco-Invitrogen. Pramipexole ((-)2-amino-4,5,6,7-tetrahydro-6-D-propylamino-benzathiazole dihydrochloride), SND919CL2x ((+)2-amino-4,5,6,7-tetrahydro-6-L-propylamino-benzathiazole dihydrochloride) and EUK-134 (manganese 3-methoxy-N,N'-bis(salicylidene)ethylenediamine chloride) were provided by Boehringer-Ingelheim. All other reagents were purchased from Sigma-Aldrich in the highest purity available, if not stated otherwise.

Cell Culture

Astroglial cells. Brains of rat pups (1-3d) were removed and dissociated with 1 % trypsin/0.05 % DNase in Hanks' balanced salt solution (HBSS) for 30 minutes at 37 °C. After addition of fetal calf serum-containing culture media, the cells were dissociated by triturating using a Pasteur pipette and centrifuged for 5 min at 300 x g. Afterwards the cells were resuspended in culture media (Dulbecco's modified Eagle media, DMEM; 10 % (v/v) heat-inactivated fetal calf serum, 6 mM L-glutamine, 100 U/ml penicillin, 100 µg/ml streptomycin, 2.5 mg/l amphotericin) and 2 x 10^5 living cells/well were seeded in 24-well plates. The cells were incubated at 37 °C, 5 % CO_2 for 14-21 days before performing experiments. Culture media was changed twice a week.

Cerebellar granule cells were isolated from 7 days old rat pups and were purified by density sedimentation. Briefly, cerebella were removed and dissociated with 1% trypsin/0.05 % DNase in HBSS for 13 min at room temperature. After two washing steps with HBSS to dilute trypsin, 0.5 % DNase in HBSS was added and the cerebella were dissociated by triturating using a Pasteur pipette. The cells were subsequently centrifuged for 15 min at 1300 x g through a 40 % (v/v) Percoll solution to separate them

from larger cell types. The cells were harvested from the pellet and washed in ice-cold Basal modified Eagle medium, supplemented with 2 mM glutamine followed by centrifugation for 5 min at 150 x g. The cells were plated on poly-L-lysine-coated 24-well plates, in BME supplemented with 10% heat-inactivated fetal calf serum, 25 mM KCl, 100 U/ml penicillin and 100 µg/ml streptomycin. After 24 h in culture, the cells were treated with cytosine arabinoside in a final concentration of 5 µM. Cultures were maintained at 37°C, 5% CO_2 for 7-8 d without a change in medium, before performing experiments.

HT-22 cells (hippocampal neuroblastoma cells derived from mice) were cultured routinely in DMEM (10 % fetal calf serum, 100 U/ml penicillin, 100 µg/ml streptomycin), 5 % CO_2, 100 % humidity. 2 x 10^4 cells were seeded into a 96-well plate and left for 16 hours to grow to 80 % confluence. This was followed by incubation in culture medium with 5 mM glutamate, with or without the additional presence of PPX, SND (both 0.008-1 mM) or EUK-134 (2-250 µM) for 24 hours. Subsequently, cell survival was assessed by the capacity of cells to reduce Alamar Blue (Serotec, 10% in culture medium, incubation for 1 hour) to resorufin, using a Fluoroskan Ascent fluorescence plate reader (Labsystems). The wavelengths for excitation and emission were set at 530 and 590 nm, respectively. The obtained fluorescence values were normalized to that obtained from untreated cells (% control). The cells were a kind gift from P. Maher (The Scripps Research Institute, La Jolla).

Preparation of brain mitochondria. 4-12 male C57BL 6 mice (20–25 g in weight; 5-6 months) were used for the preparation of forebrain mitochondria according to a modified method of Sims (Sims, 1990). The mice were fasted overnight and sacrificed by decapitation. All steps were performed at 4 °C. After rapid isolation of the brain and

dissection of the cerebella the remaining forebrains were washed in isolation buffer (210 mM mannitol, 70 mM sucrose, 1 mM EDTA, 5 mM HEPES, pH 7.4) to remove blood. The forebrains were sliced and homogenized in 10 % (w /v) isolation buffer with a teflon-in-glass potter (8 strokes, 750 rpm). The homogenate was centrifuged for 4 min at 1400 x g. The supernatant was transferred to another tube and the pellet was homogenized and centrifuged as above. The residual pellet was discarded and the pooled supernatants were centrifuged for 5 min at 30,700 x g. The pellet was resuspended in 3 ml of 15 % (v/v) Percoll in HES-buffer (5 mM HEPES; 1 mM EDTA; 0.32 M sucrose; pH 7.4) and layered on the top of a discontinuous 25-40 % (v/v) Percoll/HES-gradient (3.5 ml each). The Percoll-gradient was centrifuged for 5 min at 30,700 x g and the interphase (between 25 % and 40 % Percoll) diluted 1:4 with EDTA-free isolation buffer and centrifuged for 10 min at 16,700 x g. The supernatant was discarded and the pellet was washed once more in EDTA-free isolation buffer and centrifuged for 10 min at 7,300 x g. The resulting pellet was resuspended in 20-30 µl per mice forebrain in EDTA-free isolation buffer (about 20 mg of protein/ml). All subsequent experiments were performed within 4 h after isolation, where the mitochondria were strictly coupled and possessed a respiratory control ratio of 6, if malate/pyruvate were used as substrates. Contamination of cytosol, by determination of lactate dehydrogenase in the homogenate and the mitochondria, was about 8 %.

Uptake experiments (cells). All steps were carried out using 37°C prewarmed solutions, if not stated otherwise. For analyzing uptake of [^{3}H] PPX (Amersham Pharmacia, Freiburg; 69 mCi/mmol) the astroglial cells were washed twice with 500 µl incubation buffer (20 mM Hepes,145 mM NaCl, 1.8 mM $CaCl_2$, 5.4 mM KCl,1 mM $MgCl_2$, 0.8 mM Na_2HPO_4, 5mM glucose (Glc), pH 7.4). Afterwards the cells were preincubated

for 10 min in 200 µl incubation buffer containing Glc (10 mM) and/or inhibitors. Uptake of [^{3}H] PPX was started by addition of 200 µl [^{3}H] PPX (6 µCi/ml) in incubation buffer with or without unlabeled PPX (0-30 mM). The incubation was terminated by exhausting the incubation buffer following a washing step with 600 µl ice-cold incubation buffer. The cells were lyzed with 300 µl NaOH (1 M) for 1 h at 22°C. The alkaline lysate was neutralized with 2 M HCl and radioactivity was determined by liquid scintillation counting in a LS-3801 Beckmann-Coulter Counter. The cerebellar granule cells were incubated with the same protocol with the exception of the incubation buffer (20 mM Hepes, 5.6 mM NaCl, 1.8 mM $CaCl_2$, 145 mM KCl, 1 mM $MgCl_2$, 0.8 mM Na_2HPO_4, 5 mM Glc, pH 7.4). The uptake of [^{3}H] PPX was calculated by subtracting the obtained amount of radioactivity in the absence of cells, from the amount in the presence of cells. The concentration of [^{3}H] PPX added to the incubation medium was 43.5 nM, calculated by taking the radioactive concentration as well as the specific radioactivity of the used [^{3}H] PPX stock into account (1 mCi/ml, 69 Ci/mmol). The obtained values were normalized to the protein content and expressed in dpm/mg. The data represented correspond to the mean ± SD of 3 independent experiments.

Uptake experiments (mitochondria). All steps were carried out at 22 °C if not stated otherwise. For measuring uptake of [^{3}H] PPX; 50 µl of mitochondria (0-1.6 mg/ml) were preincubated for 2.5 min in incubation buffer (100 mM KCl,100 mM sucrose,10 mM Tris,1 mM $MgCl_2$, pH 7.4) containing energy substrates and/or mitochondrial inhibitors. Uptake of [^{3}H] PPX was started by addition of 200 µl [^{3}H] PPX (6 µCi/ml) in incubation buffer with or without unlabeled PPX (0-30 mM). The incubation was terminated after 2 min if not stated otherwise, by exhausting the incubation buffer with a cell harvester over a filter mate following a washing step with 200 µl ice-cold incubation buffer. Afterwards

the filter was dried and fused with a Meltilex sheet in the microwave. Radioactivity was determined by scintillation counting in a 1450 MicrobetaPlus liquid scintillation counter (Wallac). The specific uptake of [^{3}H] PPX was determined as the amount of radioactivity in the presence of mitochondria from which the amount of radioactivity in vigorously sonicated mitochondria was subtracted. The data represent mean ± SD of 3 independent experiments.

Hydrogen peroxide was measured using the Amplex Red™ -horseradish peroxidase method (Molecular Probes). Horseradish peroxidase (HRP) catalyzes the H_2O_2-dependent oxidation of non-fluorescent Amplex Red (AR) to fluorescent resorufin (Zhou et al., 1997). Since HRP does not cross membranes, the assay only detects H_2O_2 which has been released from the mitochondria. The reaction was started by addition of mitochondria (0.1 mg/ml) to a mixture containing Amplex Red (10 µM), HRP (0.4 U/ml) and succinate (2.5 mM; control) in incubation buffer (see uptake experiments). In further conditions PPX (300 µM), malonate (Malo, 10 mM), the SOD-Catalase mimic EUK-134 ((Melov et al., 2001), EUK, 30 µM) or ATP (1 mM) were added . Fluorescence intensity was measured in the kinetic mode, using the fluorescence plate reader as described above. The rate of resorufin generation was measured each 5 sec for a total time of 5 min and normalized to the control incubation after linear regression of the obtained fluorescence intensities. The data represent mean ± SD from 3 independent experiments. $^{*}p<0.05$, $^{**}p<0.01$, $^{***}p<0.001$ compared with the control incubation.

In a further set of experiments hydrogen peroxide (about 80 %) and, to a smaller extent superoxide (about 20 %), were generated by xanthine oxidase (0.3mU/ml) and hypoxanthine (0.1mM) (Fridovich, 1970) in a solution containing PPX, SND or EUK-134

JPET Fast Forward. Published on September 27, 2005 as DOI: 10.1124/jpet.105.092312
This article has not been copyedited and formatted. The final version may differ from this version.

at the indicated concentrations. After 20 min, ROS-generation was stopped by addition of allopurinol (1mM) and the non-detoxified H_2O_2 was detected by addition of AR and HRP (10 µM, 0.4 U/ml). Fluorescence of generated resorufin was determined in the end-point mode. The obtained values were normalized to the amount of resorufin generated in the absence of detoxifying molecule. The specificity for hydrogen peroxide was verified with SOD (300 mU/ml) which did not affect the oxidation of Amplex Red. The data represent mean ± SD from 3 independent experiments. $^{*}p<0.05$, $^{**}p<0.01$, $^{***}p<0.001$ compared with the incubation in absence of antioxidants.

NO was generated in vitro by addition of 100 µl of the NO donor (Z)-1-[2-(2-Aminoethyl)-N-(2-ammonioethyl)amino]diazen-1-ium-1,2-diolate (DETA; 0.1 and 0.3 mM) to 100 µl of a solution containing 4,5-Diaminofluorescein (DAF; 5 µM) and PPX or SND. The generation of DAF-triazole fluorescence was measured at RT every 30 s during 30 min. The obtained slopes were plotted against the concentration of PPX. The data represent mean ± SD of a representative experiment each done in triplicates

Animals

All procedures required were approved by the local ethics committee for animal experimentation. The animals were handled according to the German laws for animal experimentation. The mice were housed in groups of 4 (C57BL6 mice purchased from Janvier) or individually (SOD1-G93A mice) under standardized conditions (temperature 21°C, relative humidity 55%, 12-h light: 12-h dark cycle, lights on at 07.00 a.m.) and maintained under *ad libitum* food and water throughout the experiments. Male Tg(SOD1-G93A)1Gur/J and female B6SJLF1/J mice were obtained from Jackson Laboratories.

Mice were cross-bred and first generation offspring were screened for presence of the transgene (tail biopsy) according to Jackson Laboratories homepage (http://jaxmice.jax.org/).

Treatment of Animals

Schedule for plasma and brain levels of SND and PPX. Male C57BL/6 mice (weighing 25–30 g) were treated twice daily (7 a.m., 7 p.m.) with PPX or SND (4 in each group; 200 mg/kg) via the *per os* route for 4 consecutive days. On day 5, the animals were sacrificed 12 hours after the last treatment. Blood was collected, anticoagulated with EDTA, centrifuged to obtain plasma and stored at −20°C. Brains were rapidly removed, blotted with paper to remove excess surface blood and stored at −20°C.

Schedule for aconitase activity. Male C57BL/6 mice (weighing 25–30 g) received two intraperitoneal injections (9 a.m., 5 p.m.) of PPX (30 mg/kg, n= 8) or vehicle (water, n=6), for 4 consecutive days. On day 4 a further injection was given (9 a.m.) and 30 min later the animals were sacrificed and mitochondria were isolated as described above.

Schedule of SOD1-G93A mice: Animals were treated by supplementing the diet with PPX or SND. This minimizes stress caused by a chronic treatment (e.g. *i.p.* injection) and, due to the continuous intake, lowers peak dose effects. Only transgenic animals (SOD1-G93A) 1Gur/J D) were included in the study. Group I (6 males, 5 females) obtained control diet (altromin Granulat 8/15; Altromin 32770 Lage/Lippe, Deutschland) and water, group II (7 males, 8 females) obtained control diet and PPX in the drinking water (3 mg/kg/day), group III (6 males, 9 females) obtained SND in the diet (100 mg/kg/day) and water. Consumption of drinking-water and pellets was tested in regular intervals of 7 days. Drug administration started at day 45 and was continued until removal of the animal from the study. To assess the effects of the drug treatment, the

lifetime of each animal was recorded (date of birth until removal from the study or death of the animal) and compared by Kaplan-Meier survival analysis followed by Logrank Mantel-Cox test.

Motor activity of SOD1-G93A mice was assessed by monitoring the running-wheel activity of each mouse. It correlates directly with the revolutions per minute (rpm) generated by each animal in the running-wheel. At day 38 (age), the animals were placed into cages equipped with a running-wheel. Running-wheel activity of each mouse was recorded for 12 hours from 8 p.m. to 8 a.m. each day. Analysis of the data was accomplished using a program supplied by LMTB Berlin (Maus Vital). Animals were removed from the study if they reached disease end-stage, characterized by running-wheel activity less than 10 rpm/12 hours or disability to rise within 30 seconds.

For the evaluation of activity, performance values were averaged within the treatment groups for each day of age. The resulting time-performance values for each treatment group were fitted by the 3 parametric sigmoidal curve ($f(x)= ax^c/ (x^c+ b^c)$, in which “a” represents the upper asymptote and therefore presymptomatic performance, “b” the day of half maximum performance, and “c” the disease progression as the decline of running wheel activity per day. The fit parameters and 95% confidence intervals of the fit parameters were calculated by means of non-linear regression. The treatment groups were compared by these fit parameters. A statistically significant difference between two treatment groups according to a fit parameter was achieved if the 95% confidence intervals of the fit parameters did not overlap. The statistical evaluation was performed using the software package SAS Version 8.2.

Post-mortem analysis

JPET Fast Forward. Published on September 27, 2005 as DOI: 10.1124/jpet.105.092312
This article has not been copyedited and formatted. The final version may differ from this version.

Plasma and brain levels of PPX or SND. For quantification of PPX or SND in brain the tissue was homogenized with 0.05 M phosphoric acid. An aliquot of the homogenate was spiked with standard solutions or water and internal standard and then extracted two times with tert.-butyl-methylether at pH 10. Plasma samples were diluted with standard solutions or water and an internal standard and then extracted two times with tert.-butyl-methylether at pH 10. The extracts were evaporated under dry nitrogen at 40°C and reconstituted with a mixture of methanol/water/formic acid (27/75/0.1). All extracts were diluted prior to analysis to fit into the calibrated concentration range. This solution was injected into the LC/MSMS system consisting of an Agilent 1100 HPLC-system and a API4000 mass spectrometer (Applied Biosystems). Chromatography took place on a Kromasil RP18 column (2.1 mm ID x 30 mm, 5 µm particle size) with a gradient from 0.1 % formic acid in 10mM ammonium acetate to 0.1 % formic acid in acetonitrile/water (90/10 (v/v)) in 4 minutes. Samples and internal standard were detected by ESI-MSMS in multiple reaction monitoring mode. The limit of quantification was 2nM. For both analytes a linear calibration range from 2 to 4000 nM was observed. Shown results are mean ± SEM of 4 animals.

Mitochondrial aconitase is reversibly inactivated by superoxide and has therefore been used as a marker for steady-state concentration of superoxide *in vitro* and *in vivo* (reviewed by (Tarpey et al., 2004)). Mitochondrial aconitase activity was measured by the method of (Gardner et al., 1994), which was slightly modified. Mitochondria (about 10 mg/ml) were diluted in lysis buffer containing 10 mM Tris/HCl, 0.6 mM $MnCl_2$, 20 µM D/L- fluorocitrate, 1 % (v/v) Triton X-100 pH 7.4 and incubated for 30 min on ice. 20 µl of lysate was added to a well of a 96 well microtiter plate, followed by the addition of a prewarmed solution (37°C) containing 0.4 mM NADP, 1.2 mM $MnCl_2$, 2 U/ml isocitrate

dehydrogenase in buffer (10 mM Tris/HCl, 0.6 mM $MnCl_2$, 20 µM D/L- fluorocitrate, 1 % (v/v) Triton X-100). After 5 min preincubation the generation of NADPH was started by addition of 10mM citrate in buffer. The increase in absorbance was followed each 15 sec for a period of 10 min in an iEMS plate reader (Labsystems). Aconitase activity was calculated by using an absorbance coefficient of 6.22 mM^{-1} x cm^{-1} for NADPH and a thickness of 0.5 cm for 200 µl in the well, which was normalized to the protein content afterwards.

Additionally a monoclonal antibody raised against the 23 C-terminal amino acids of aconitase-2 (mitochondrial aconitase) from rat (nanoTools Antikörpertechnik, Teningen, Germany) was used to study the expression of the protein in mitochondria. This antibody (Clone 29 A4) recognizes a single band with an apparent mass of about 82 kD in human A431 cells as well as mouse and rat forebrain mitochondria. For Western blotting, equal amounts of mitochondrial lysates (5 µg) were reduced with dithiothreitol and subjected to SDS/PAGE on a 10% polyacrylamide gel. Afterwards aconitase-2 expression was analyzed by a standard Western blot protocol by probing the used nitrocellulose membranes with the anti-aconitase-2 antibody (2 µg/ml) using an enhanced chemiluminescence detection system (Applied Biosystems).

Presentation of data and statistical analysis: All *in vitro* experiments were carried out on at least three independent cell cultures or mitochondrial preparations. For experiments performed *in vivo*, each individual animal was regarded to represent an independent experiment. Therefore the results are presented as mean values ± SD of n experiments *in vitro*, or as mean values ± SEM of n animals when performed *in vivo*. In the figures the bars have been omitted if they were smaller than the symbols representing the mean values. If not stated otherwise, multiple comparisons of data

were analyzed by ANOVA followed by the Bonferroni post hoc test, using SigmaStat Vers. 2.03. A *p*-value of <0.05 was considered statistically significant.

Results

To test for an intracellular site of action, uptake of [^{3}H] PPX into neural cells, both cerebellar granule cells and astroglial cells, was examined. Uptake of PPX increases with incubation time and reaches constant levels after incubation for 20 min (figure 1 A). After reaching plateau, the amount of [^{3}H] PPX obtained in the cell lysates does not differ significantly between neurons (0.7 ± 0.2 pmol/mg) and astroglial cells (0.60 ± 0.09 pmol/mg). Additionally the amount in astroglial cells converts to an intracellular concentration of 160 nM [^{3}H] PPX, by taking the specific volume for astroglial cells (4 µl/mg protein) into account (Dringen and Hamprecht, 1998).

In both cell types (figure 1 B), uptake is inhibited to about 10 - 20 % in digitonin permeabilized cells and by acidification (pH 6) compared to the incubation at pH 7.4. In contrast to acidification, an increase to pH 8 doubles PPX influx in both cell types, compared to pH 7.4.

Dilution of [^{3}H] PPX with unlabeled PPX, results in a dose-dependent inhibition of [^{3}H] PPX uptake (figure 1 C), which is caused by isotope dilution as shown in figure 1 D. Multiplication of [^{3}H] PPX-uptake (figure 1 C) by the molar excess of unlabeled PPX yields the rate of total PPX-uptake (labeled plus unlabeled; figure 1 D), which is proportional to the total PPX concentration (labeled plus unlabeled) over a range of seven orders of magnitude (figure 1 D).

In a second set of experiments, entry of PPX into isolated mitochondria was measured and characterized. As observed in cells, uptake of [^{3}H] PPX in mitochondria strongly

depends on mitochondrial integrity (figure 2 A), as disruption of mitochondria by vigorous sonication or Triton X-100 results in a significant inhibition to about 15 % (figure 2 A). In intact mitochondria uptake reaches maximal values after 5 min in the presence of energy substrates malate plus pyruvate. By subtraction the amount of [^{3}H] PPX for unspecific binding (sonicated mitochondria), from the amount obtained in intact energized mitochondria, a specific uptake of 0.15 ± 0.01 pmol [^{3}H] PPX per mg protein is obtained, which corresponds to an intramitochondrial concentration of 150 nM by accounting for a mitochondrial volume of 1 µl/mg (Halestrap and Quinlan, 1983).

Furthermore, [^{3}H] PPX uptake is proportional to the mitochondria amount (R^2 = 0.971; figure 2 B) and depends on the intramitochondrial volume (figure 2 C), which was modified by using hypo- or hypertonic buffers, respectively. Uptake is significantly increased in conditions of mitochondrial swelling (hypotonic buffer), and *vice versa* significantly inhibited in hypertonic buffer (both, $p < 0.001$). As observed in cells, mitochondrial uptake of [^{3}H] PPX is significantly inhibited in the presence of unlabelled PPX (> 1 µM, data not shown) which after taking the molar excess of unlabeled into account, results in a linear relationship between the rate of total uptake (labeled plus unlabeled) and the total PPX concentration (R^2 = 0.999; figure 2 D).

To evaluate the membrane potential as a driving force for mitochondrial [^{3}H] PPX uptake, we used different energy substrates to polarize the mitochondrial membrane as well as different inhibitors to depolarize it (figure 2 E). Any of the used energy substrates (malate/pyruvate, succinate or ATP) result in a comparable [^{3}H] PPX-uptake. Withdrawal of these substrates in turn reduces uptake to about 20% ($p<0.001$). Furthermore, uptake

in malate/pyruvate energized mitochondria is significantly inhibited if mitochondrial membrane potential is reduced by addition of ADP+Pi (57%), valinomycin (47%), calcium + Pi (44%), rotenone (41%), or FCCP (27%), respectively.

After demonstrating entry of PPX into brain cells and mitochondria, we re-evaluate the antioxidative properties of PPX and SND and compare the obtained efficacy with EUK-134, a potent SOD/Cat-mimetic (Melov et al., 2001).

First, H_2O_2 and superoxide were generated by xanthine oxidase (Fridovich, 1970) in a cell-free assay, where detoxifying enzymes and membranes are absent. This allows the evaluation of the dose response for the detoxification of *in situ* generated ROS by an antioxidant, independent of its uptake properties. Additionally allopurinol was used to measure the efficacy of the antioxidant without the competition between antioxidant and the detection system.

As expected EUK-134 was the most potent compound, which at a concentration of 300 µM, is able to detoxify more than 95% of ROS, generated by xanthine oxidase. Both PPX and SND are less potent at this concentration (about 75% residual H_2O_2), however, a dose dependent effect for detoxifying hydrogen peroxide by both enantiomers is observed (figure 3 A). Comparable ROS-detoxification is achieved at 3 µM EUK-134 and 1 mM for either PPX or SND. Additionally both enantiomers show equipotent efficacy in detoxification of xanthine oxidase generated ROS (figure 3 A).

To show that PPX and EUK-134 are able to inhibit mitochondrial hydrogen peroxide release, we measured release of hydrogen peroxide in succinate-energized mitochondria in the presence of PPX (300 uM) or EUK-134 (30 uM). Both compounds significantly inhibit the release of hydrogen peroxide to 73% and 58% respectively, compared to the values obtained in the absence of an antioxidant (Ctrl, figure 3 B).

To evaluate if these antioxidative properties of PPX and SND are sufficient to confer neuroprotection in a cellular model of oxidative stress qualitatively, HT-22 cells were treated with glutamate to induce cell death (figure 3 C). HT-22 cells have been shown to be particularly sensitive to glutamate toxicity, which involves a glutamate/cysteine antiporter: high extracellular levels of glutamate deplete the cells of cysteine, causing a decrease in cellular glutathione (and not the activation of glutamate receptors). This has been described to result in an early increase of ROS (5-10-fold), followed by a later but massive increase in ROS (200-400-fold) derived from mitochondria and paralleled by the time of cell death (Tan et al., 1998).

In our hands, treatment of HT-22 cells with glutamate results in oxidative stress after 8 hours of incubation, as observed by an increased oxidation of dihydro-2,7-dichloro-fluorescein-diacetate to the fluorescent 2,7-dichloro-fluorescein (data not shown). After a 24 hour exposure to glutamate, cell viability was reduced to 13 ± 8 % ($^{###}p < 0.001$, compared to untreated cells, figure 3 C). In the absence of glutamate, incubation with PPX or SND (both at 1 mM) do not significantly affect cell viability, whereas EUK-134 (at 250 µM) reduces cell viability to 64 ± 8 % ($^{#}p < 0.05$, compared to untreated cells). PPX, SND and EUK were able to prevent glutamate induced cell death (***p < 0.001 for all

three compounds). Protection up to 82 % remaining viability occurred at 1 mM (PPX and SND) and 250 µM (EUK-134). PPX, SND and EUK-134 were able to protect cells in a dose-dependent manner (data not shown). EC_{50} concentrations were determined by non-linear regression as 370 ± 50 µM, 190 ± 80 µM and 20 ± 1 µM, respectively (data given as mean ± SD of 8 independent experiments). Multiple comparison of the obtained EC_{50} concentrations by ANOVA followed by Bonferroni's post-hoc test resulted in no significant difference between PPX and EUK.

Since H_2O_2 decomposes within hours (Halliwell, 1999) we focused on the more reactive radical nitric oxide generated by the nitric oxide-donor DETA, which in the presence of 4,5-diaminofluorescein (DAF) yields the fluorescent DAF-triazole. Both PPX and SND (figure 4) equally inhibit the generation of the DAF triazole. The IC_{50} values determined by non linear regression for both enantiomers are 15 ± 2 µM (mean ± sd of 3 independent experiments).

To confirm whether the *in vitro* data have relevance *in vivo*, we tested if micromolar concentrations of PPX and SND can be achieved *in vivo*. We treated C57BL6 mice with high doses of PPX and SND (200 mg/kg, p.o. for 4 days) and determined plasma and brain levels 12 hours after the last treatment. Table 1 a shows that micromolar concentrations in the brain are achieved for both enantiomers. Further, the brain levels are at least six-fold higher than those obtained in plasma.

This was followed by an experiment where mitochondria were isolated after PPX-treatment of mice to determine mitochondrial aconitase activity, an indicator for steady

state levels of superoxide (Tarpey et al., 2004). PPX treatment for 4 days (2 x 30 mg/kg) increased mitochondrial aconitase activity by 42 % to 67 ± 16 mU/mg compared to vehicle treated animals (47 ± 9 mU/mg, figure 5 A). This was not due to altered expression of mitochondrial aconitase, as protein levels were not affected by the PPX-treatment (figure 5 B).

Consequently we tested both compounds in mice expressing the G93A-mutant SOD1, a common and well-described model of ALS, where neuronal cell death is associated with an increase in oxidative stress and mitochondrial alterations (Menzies et al., 2002; Bendotti and Carri, 2004).

We confirmed that in this mouse model, and in the dosage regimen intended for the animal trial (long term, continuous *per os* application), meaningful plasma levels can be achieved. A dose-response for SND application and resulting plasma levels is demonstrated in Table 1 b. Application of 100 mg SND/kg/day resulted in plasma levels of 160 nM SND, which -based on our brain accumulation data- was predicted to result in brain levels within the micromolar range.

Since we found equipotent antioxidative properties of PPX and SND, and no evidence for a transporter which is involved in the uptake of PPX, we tested SND at a high dose of 100 mg/kg, to achieve antioxidative action. PPX was given at a lower dose of 3 mg/kg (shown to be neuroprotective in models of dopaminergic neurodegeneration (Zou et al., 2000; Anderson et al., 2001)), to test for putative neuroprotection in the ALS-model, which might be mediated via activation of dopamine receptors.

Regarding basal running-wheel activity (or presymptomatic performance), there is no significant difference between SND treated animals (14700 rpm/12 hours [14200-15200]) and the control group (15400 rpm/12 hours [14600 – 16200]; figure 5 A, [95% confidence interval]). In contrast, PPX treated animals show a significant increase by 55% to 23900 rpm/12 hours [23200 – 24600] in presymptomatic running-wheel activity compared to the SND treated animals and the control group.

No significant differences are obtained for the slopes in the inflection point of the motor performance curve (see parameter c, in methods), which ranged from -18 to -24 rpm/d between the different groups. In contrast, the time-point of half-maximal motor performance occurs at day 103 [102 – 104] in vehicle treated animals, which occurs significantly delayed at day 106 [105 – 106] or 109 [108 – 110] in PPX- or SND treated animals, respectively.

Additionally, survival time in SND treated SOD1 (G93A) mice (132 ± 2 days, mean ± SEM, n = 15) is significantly prolonged compared to the control group (125 ± 2 days, logrank test p = 0.011, mean ± SEM, n = 11), and in comparison to the PPX treated group (122 ± 2 days, logrank test p = 0.002; mean ± SEM, n = 15). The survival times of the PPX treated animals and the control group do not differ significantly (Logrank Mantel-Cox test, p=0.464; figure 5 B).

Discussion

PPX has been proposed to accumulate in mitochondria (Abramova et al., 2002). Since cellular uptake is a prerequisite for penetration into mitochondria, we show that [^{3}H]-PPX enters astrocytes and neurons beyond non-specific binding, indicated by reduced uptake in digitonin-permeabilized cells. Furthermore [^{3}H]-PPX accumulates in astroglial cells as shown by the 3-fold intracellular concentration compared to incubation buffer. The mechanism of uptake is not transporter-mediated and therefore diffusion-limited, due to the non-saturable rate of total PPX uptake (labeled plus unlabelled) which is proportional to the total PPX concentration.

The increase in cellular uptake by alkalinisation and inhibition by acidification might be explained by the pK-values of PPX (about 5 and 11 for the aminothiazole- and propylamino-group, respectively). At pH 7.4, more than 98% of PPX is protonated to the less permeable univalent cation; a pH increase raises the concentration of the neutral molecule, which penetrates the cells more easily than the protonated species.

Mitochondrial [^{3}H]-PPX uptake is proportional to mitochondrial amount and correlates with the intra-mitochondrial volume, since mitochondrial swelling or shrinkage result in an increase or a decrease in uptake, respectively. The ability of mitochondria to retain [^{3}H]-PPX is greatly affected by rupture of the mitochondrial membranes, showing that non-specific binding of PPX to mitochondrial proteins is low. We conclude that PPX permeates the inner mitochondrial membrane and enters the matrix.

As in cells, mitochondrial uptake is not transporter-mediated, but depends on mitochondrial membrane potential. We show that in energized mitochondria [^{3}H]-PPX-influx is stimulated by a factor of two to six, irrespective of the energy substrate used, compared to all conditions where generation of a membrane potential was prevented. The obtained intramitochondrial concentration of 150 nM in energized mitochondria accounts for a threefold accumulation of PPX within mitochondria compared to incubation buffer. The obtained values in FCCP depolarized mitochondria (0.06 pmol/mg) most likely reflect the uniform distribution of PPX between incubation buffer and mitochondrial matrix (diffusion only), whereas in energized mitochondria (0.15 pmol/mg) uptake of the cation is driven additionally by the membrane potential (negative inside).

The results are consistent with the accumulation of lipophilic cations in mitochondria, driven by the mitochondrial membrane potential (reviewed by Ross et al., 2005). Additionally the model of Trapp and Horobin (2005) predicts the accumulation of strong bases (non-permanent cations like PPX; pK_2 about 11), in energized mitochondria, if hydrophobicity, needed for membrane penetration, is given by an equal octanol/water partitioning (log P= 0, PPX about -0.2, data not shown).

We conclude that apart from its binding to dopamine receptors, PPX can accumulate within cells and mitochondria. We assume that SND enters cells and mitochondria by the same mechanism, as no transporter is involved, and the chiral configuration of the aminopropylgroup does not affect the physico-chemical determinants for uptake (pK-values and hydrophobicity).

Although several studies addressed the antioxidative properties of PPX (e.g. Cassarino et al., 1998; Ferger et al., 2000), its efficacy might have been underestimated due to the efficient and competing detection systems (Floyd et al., 1984). Therefore we re-evaluate the antioxidative properties of PPX and SND targeted towards different reactive species and compartments; obtained efficacies were compared to EUK-134, a potent SOD/Catalase-mimetic (Jung et al., 2001; Melov et al., 2001).

We show that PPX and (the equipotent) SND are weak H_2O_2 scavengers, if generation and detoxification are measured in the same compartment, in absence of a detection system (xanthine oxidase). In contrast, EUK-134 detoxifies the generated ROS in the 5 µM range, indicating 100-fold higher efficacy compared to PPX or SND. However, the efficacy of EUK-134 decreased by a factor of five in presence of a detection system (mitochondrial H_2O_2 release) or in HT-22 cells, where cell death was induced by glutathione depletion (Murphy et al., 1989; Tan et al., 1998). Importantly, loss of efficacy was not observed if PPX or SND were tested in these systems.

This is consistent with the uptake properties of PPX, yielding cellular or mitochondrial accumulation, thus bypassing competition with the detection system (mitochondrial H_2O_2-release) and exerting inhibition of cell death at even lower concentrations (IC_{50} at 300 µM). The uptake properties and the efficacy of PPX to scavenge H_2O_2 (accumulates 3-fold, IC_{50} for H_2O_2 about 1 mM) are sufficient to explain its neuroprotection in glutathione-depleted HT-22 cells (EC_{50} about 300 µM). Additionally, the equipotent efficacy of SND to protect HT-22 cells indicates a dopamine-receptor independent

mechanism and is consistent with the assumption that SND enters cells and mitochondria. Mitochondrial ROS attenuation in HT22 cells is sufficient but not a prerequisite to protect HT-22 cells from cell death. Therefore, pathways by PPX/SND other than antioxidative action located to mitochondria cannot be excluded. However, alternative pathways were not examined in this paper.

The low efficacy of PPX and SND towards H_2O_2 might be due to its low reactivity (Halliwell, 1999). Therefore we evaluate the efficacy for more reactive species: nitric oxide or superoxide (both decompose within seconds). The inhibition of DAF-triazole generation in presence of a nitric oxide-donor and antioxidant (Nagata et al., 1999) was used to show that PPX and SND detoxify nitric oxide equipotently at the 15 µM level. We conclude that the antioxidative efficacy of PPX and SND, in addition to the spatial issues discussed above, depends on the reactivity of the respective radical, since the IC_{50} values for nitric oxide and H_2O_2 vary at least by a factor of 50.

We show that PPX-treatment (2x 30 mg/kg) results in an increase in mitochondrial aconitase activity *in vivo*, indicating a reduction of the superoxide steady state level within mitochondria (Tarpey et al., 2004). Since treatment of these mice with a PPX-dose of 2 x 200 mg/kg results in micromolar brain levels, even 12 hours after the last treatment, the increase in mitochondrial aconitase might result from total brain concentrations within the same order of magnitude.

Aconitase measurements were performed by (Gu et al., 2004), showing equipotent protection of mitochondria in dopaminergic and non-dopaminergic cells in the presence

of 10 µM PPX or SND, if added 48 hours prior to complex I-inhibitiors. PPX causes a slight, but not significant increase in total aconitase activity in 1-methyl-4-phenylpyridinium treated SHSY-5Y cells. We hypothesize that either we achieved higher intramitochondrial concentrations, or the protective effects observed by Gu *et al.* are related to the preincubation, which may alter gene-expression and mediate protection by an alternative mechanism (e.g. Ling et al., 1998; Presgraves et al., 2004; Pan et al., 2005).

The present results support the concept of PPX and SND as mitochondria-targeted antioxidants, evidenced by equal antioxidative efficacy towards H_2O_2 and nitric oxide, and equipotent efficacy in preventing cell death in glutathione-depleted cells. Targeting of PPX to mitochondria is supported by the membrane potential-dependent uptake process in which no transporter is involved, by higher efficacy for cellular protection compared to “direct scavenging”, and finally by the ability of PPX to lower mitochondrial superoxide levels *in vivo*.

We conclude that the *in vitro* neuroprotective properties of PPX are independent of the chiral 6-propylaminogroup in the molecule. Therefore the (+)-enantiomer SND, rather than PPX, might permit a sufficiently high dosage regimen to exert antioxidative and neuroprotective efficacy *in vivo* without causing side effects by over-stimulation of dopamine receptors.

Therefore we tested SND (at a high dose) and PPX (at a low dose) in an animal model for familial ALS, the SOD1-G93A mice. The dose of 100 mg/kg per day for SND was

tested to achieve antioxidative action based on equipotent efficacy compared to PPX and the micromolar brain levels achieved in C57BL6 mice. The used PPX dose of 3 mg/kg per day was chosen based on the expected dopaminergic stimulation, in order to demonstrate that protection of dopaminergic neurons does not confer beneficial effects in the SOD1-G93A mouse. Indeed we show that treatment with PPX does not increase survival time of the SOD1-G93A mice and conclude that the use of a dopamine agonist does not result in meaningful neuroprotection, although loss of dopaminergic neurons has been described in these animals (e.g. Kostic et al., 1997) and in patients (e.g. Przedborski et al., 1996). PPX treated animals display an increase in presymptomatic running-wheel activity; probably a result of dopaminergic stimulation. Early after disease onset, these animals have a decreased probability of survival (from day 115 to 133). This could be indicating that the demand on muscle cells is detrimental to survival, which has been observed in other studies as well (Mahoney et al., 2004).

The high-dose treatment with SND significantly prolongs survival time and improves motor performance (indicated by a delay of half-maximal performance) by 7 and 6 days, respectively. These effects are comparable to the treatment with 30 mg/kg riluzole (the only drug launched for ALS) which prolongs survival time by 8 days in our laboratory (unpublished observation). The absence of pre-onset hyperactivity in SND treated animals suggests that the dose given does not confer dopaminergic stimulation.

Since disease progression was not altered, we conclude that SND acts as a neuroprotectant in the SOD1-G93A mice, resulting in a later onset of symptoms as well as an extended survival-time. Based on the high dose, the equipotent antioxidative

properties of PPX and SND and the lack of evidence for different distribution *in vivo* or *in vitro*, we propose that the beneficial effects of SND in the animals are mediated by SND's brain- and mitochondria-targeted antioxidative property. However, mitochondrial action of SND in the SOD1-G93A mouse needs to be confirmed by direct measurement of mitochondrial ROS attenuation in this model, using specific endpoints such as modification of mitochondrial proteins or mitochondrial aconitase activity. In summary, SND might be a structural prototype, suitable for further chemical modification, to obtain a mitochondrial targeted antioxidant with higher efficacy.

Acknowledgements

We thank M. Boehringer, S. Brezina, K. Eltges and S. Fleissner for their excellent technical assistance.

References

Abramova NA, Cassarino DS, Khan SM, Painter TW and Bennett JP, Jr. (2002) Inhibition by R(+) or S(-) pramipexole of caspase activation and cell death induced by methylpyridinium ion or beta amyloid peptide in SH-SY5Y neuroblastoma. *J Neurosci Res* **67**:494-500.

Andersen JK (2004) Oxidative stress in neurodegeneration: cause or consequence? *Nat Med* **10 Suppl**: 18-25.

Anderson DW, Neavin T, Smith JA and Schneider JS (2001) Neuroprotective effects of pramipexole in young and aged MPTP-treated mice. *Brain Res* **905**:44-53.

Bendotti, C., N. Calvaresi, L. Chiveri, A. Prelle, M. Moggio, M. Braga, V. Silani, and S. De Biasi. 2001. Early vacuolization and mitochondrial damage in motor neurons of FALS mice are not associated with apoptosis or with changes in cytochrome oxidase histochemical reactivity. *J Neurol Sci* 191 (1-2):25-33.

Bendotti C and Carri MT (2004) Lessons from models of SOD1-linked familial ALS. *Trends Mol Med* **10**:393-400.

Cassarino DS, Fall CP, Smith TS and Bennett JP, Jr. (1998) Pramipexole reduces reactive oxygen species production in vivo and in vitro and inhibits the mitochondrial permeability transition produced by the parkinsonian neurotoxin methylpyridinium ion. *J Neurochem* **71**:295-301.

Dringen R and Hamprecht B (1998) Glutathione restoration as indicator for cellular metabolism of astroglial cells. *Dev Neurosci* **20**:401-407.

Ferger B, Teismann P and Mierau J (2000) The dopamine agonist pramipexole scavenges hydroxyl free radicals induced by striatal application of 6-hydroxydopamine in rats: an in vivo microdialysis study. *Brain Res* **883**:216-223.

Floyd RA, Watson JJ and Wong PK (1984) Sensitive assay of hydroxyl free radical formation utilizing high pressure liquid chromatography with electrochemical detection of phenol and salicylate hydroxylation products. *J Biochem Biophys Methods* **10**:221-235.

Fridovich I (1970) Quantitative aspects of the production of superoxide anion radical by milk xanthine oxidase. *J Biol Chem* **245**:4053-4057.

Gardner PR, Nguyen DD and White CW (1994) Aconitase is a sensitive and critical target of oxygen poisoning in cultured mammalian cells and in rat lungs. *Proc Natl Acad Sci U S A* **91**:12248-12252.

Gu M, Irvani M, Cooper JM, King D, Jenner P and Schapira AH (2004) Pramipexole protects against apoptotic cell death by non-dopaminergic mechanisms. *J Neurochem* **91**:1075-1081.

Halestrap AP and Quinlan PT (1983) The intramitochondrial volume measured using sucrose as an extramitochondrial marker overestimates the true matrix volume determined with mannitol. *Biochem J* **214**:387-393.

Halliwell B (1999) Antioxidant defence mechanisms: from the beginning to the end (of the beginning). *Free Radic Res* **31**:261-272.

Jung C, Rong Y, Doctrow S, Baudry M, Malfroy B and Xu Z (2001) Synthetic superoxide dismutase/catalase mimetics reduce oxidative stress and prolong survival in a mouse amyotrophic lateral sclerosis model. *Neurosci Lett* **304**:157-160.

Kakimura J, Kitamura Y, Takata K, Kohno Y, Nomura Y and Taniguchi T (2001) Release and aggregation of cytochrome c and alpha-synuclein are inhibited by the antiparkinsonian drugs, talipexole and pramipexole. *Eur J Pharmacol* **417**:59-67.

Kitamura Y, Kosaka T, Kakimura JI, Matsuoka Y, Kohno Y, Nomura Y and Taniguchi T (1998) Protective effects of the antiparkinsonian drugs talipexole and pramipexole against 1-methyl-4-phenylpyridinium-induced apoptotic death in human neuroblastoma SH-SY5Y cells. *Mol Pharmacol* **54**:1046-1054.

Kostic V, Gurney ME, Deng HX, Siddique T, Epstein CJ and Przedborski S (1997) Midbrain dopaminergic neuronal degeneration in a transgenic mouse model of familial amyotrophic lateral sclerosis. *Ann Neurol* **41**:497-504.

Le WD, Jankovic J, Xie W and Appel SH (2000) Antioxidant property of pramipexole independent of dopamine receptor activation in neuroprotection. *J Neural Transm* **107**:1165-1173.

Ling ZD, Robie HC, Tong CW and Carvey PM (1999) Both the antioxidant and D3 agonist actions of pramipexole mediate its neuroprotective actions in mesencephalic cultures. *J Pharmacol Exp Ther* **289**:202-210.

Ling ZD, Tong CW and Carvey PM (1998) Partial purification of a pramipexole-induced trophic activity directed at dopamine neurons in ventral mesencephalic cultures. *Brain Res* **791**:137-145.

Maher P and Davis JB (1996) The role of monoamine metabolism in oxidative glutamate toxicity. *J Neurosci* **16**:6394-6401.

Mahoney DJ, Rodriguez C, Devries M, Yasuda N and Tarnopolsky MA (2004) Effects of high-intensity endurance exercise training in the G93A mouse model of amyotrophic lateral sclerosis. *Muscle Nerve* **29**:656-662.

Melov S, Doctrow SR, Schneider JA, Haberson J, Patel M, Coskun PE, Huffman K, Wallace DC and Malfroy B (2001) Lifespan extension and rescue of spongiform encephalopathy in superoxide dismutase 2 nullizygous mice treated with superoxide dismutase-catalase mimetics. *J Neurosci* **21**:8348-8353.

Menzies FM, Cookson MR, Taylor RW, Turnbull DM, Chrzanowska-Lightowlers ZM, Dong L, Figlewicz DA and Shaw PJ (2002) Mitochondrial dysfunction in a cell culture model of familial amyotrophic lateral sclerosis. *Brain* **125**:1522-1533.

Mierau J (1995) Pramipexole: a dopamine receptor agonist for treatment of Parkinsons disease. *Clin Neuropharmacol* **18**:195-206.

Mierau J, Schneider FJ, Ensinger HA, Chio CL, Lajiness ME and Huff RM (1995) Pramipexole binding and activation of cloned and expressed dopamine D2, D3 and D4 receptors. *Eur J Pharmacol* **290**:29-36.

Murphy TH, Miyamoto M, Sastre A, Schnaar RL and Coyle JT (1989) Glutamate toxicity in a neuronal cell line involves inhibition of cystine transport leading to oxidative stress. *Neuron* **2**:1547-1558.

Nagata N, Momose K and Ishida Y (1999) Inhibitory effects of catecholamines and anti-oxidants on the fluorescence reaction of 4,5-diaminofluorescein, DAF-2, a novel indicator of nitric oxide. *J Biochem* **125**:658-661.

Pan T, Xie W, Jankovic J and Le W (2005) Biological effects of pramipexole on dopaminergic neuron-associated genes: relevance to neuroprotection. *Neurosci Lett* **377**:106-109.

Pattee GL, Post GR, Gerber RE and Bennett JP, Jr. (2003) Reduction of oxidative stress in amyotrophic lateral sclerosis following pramipexole treatment. *Amyotroph Lateral Scler Other Motor Neuron Disord* **4**:90-95.

Presgraves SP, Borwege S, Millan MJ and Joyce JN (2004) Involvement of dopamine D(2)/D(3) receptors and BDNF in the neuroprotective effects of S32504 and pramipexole against 1-methyl-4-phenylpyridinium in terminally differentiated SH-SY5Y cells. *Exp Neurol* **190**:157-170.

Przedborski S, Dhawan V, Donaldson DM, Murphy PL, McKenna-Yasek D, Mandel FS, Brown RH, Jr. and Eidelberg D (1996) Nigrostriatal dopaminergic function in familial amyotrophic lateral sclerosis patients with and without copper/zinc superoxide dismutase mutations. *Neurology* **47**:1546-1551.

Ramirez AD, Wong SK and Menniti FS (2003) Pramipexole inhibits MPTP toxicity in mice by dopamine D3 receptor dependent and independent mechanisms. *Eur J Pharmacol* **475**:29-35.

Ross MF, Kelso GF, Blaikie FH, James AM, Cocheme HM, Filipovska A, Da Ros T, Hurd TR, Smith RA and Murphy MP (2005) Lipophilic triphenylphosphonium cations as tools in mitochondrial bioenergetics and free radical biology. *Biochemistry* **70**:222-230.

Sims NR (1990) Rapid isolation of metabolically active mitochondria from rat brain and subregions using Percoll density gradient centrifugation. *J Neurochem* **55**:698-707.

Tan S, Wood M and Maher P (1998) Oxidative stress induces a form of programmed cell death with characteristics of both apoptosis and necrosis in neuronal cells. *J Neurochem* **71**:95-105.

Tarpey MM, Wink DA and Grisham MB (2004) Methods for detection of reactive metabolites of oxygen and nitrogen: in vitro and in vivo considerations. *Am J Physiol Regul Integr Comp Physiol* **286**:R431-444.

Trapp S and Horobin RW (2005) A predictive model for the selective accumulation of chemicals in tumor cells. *Eur Biophys J*.

Xu Z, Jung C, Higgins C, Levine J and Kong J (2004) Mitochondrial degeneration in amyotrophic lateral sclerosis. *J Bioenerg Biomembr* **36**:395-399.

Zhou M, Diwu Z, Panchuk-Voloshina N and Haugland RP (1997) A stable nonfluorescent derivative of resorufin for the fluorometric determination of trace hydrogen peroxide: applications in detecting the activity of phagocyte NADPH oxidase and other oxidases. *Anal Biochem* **253**:162-168.

Zou L, Xu J, Jankovic J, He Y, Appel SH and Le W (2000) Pramipexole inhibits lipid peroxidation and reduces injury in the substantia nigra induced by the dopaminergic neurotoxin 1-methyl-4-phenyl-1,2,3,6-tetrahydropyridine in C57BL/6 mice. *Neurosci Lett* **281**:167-170.

Legends for Figures

Figure 1: Uptake of [³H]-PPX in neural cells. Uptake in astroglial cells (opened circles/bars) or cerebellar granule neurons (filled circles/bars) was started by addition of [³H]-PPX (3 µCi/ml) in incubation buffer containing 5 mM Glc and terminated at the indicated time (**A**) or after 10 min (**B-D**). In (**B**) uptake was modulated at 37°C by using an incubating buffer pH 7.4 (Ctrl), containing Digitonin (Digi, 100 µg/ml) or adjusting the pH to 6 or 8, respectively. In (**C, D**), uptake was started by addition of [³H]-PPX (3 µCi/ml) and a variable concentration of unlabeled PPX (0-30mM). **C**: Uptake was normalized on time and expressed as rate of [^{3}H]-PPX uptake. **D**: The specific rate of total PPX uptake was calculated by taking the excess of unlabeled PPX into account and is shown as a function of total PPX concentration in the incubation buffer. *p<0.05, **p<0.01, ***p<0.001 compared to (**B**) the control incubation for a given cell type, or (**C**) the incubation in the absence of unlabeled PPX, respectively.

Figure 2: Uptake of [^{3}H] PPX in mitochondria. Mitochondria (control; open circles, bars), were lysed (Triton-X 100;1% (v/v); open triangles), sonicated vigorously (SMP; filled triangles) or uncoupled with FCCP (1 µM; filled circles) and preincubated for 2.5 min in malate/pyruvate–containing (2.5/5 mM) incubation buffer (all 0.2 mg/ml). Uptake was started by addition of [³H] PPX (3 µCi/ml) and terminated at the indicated time (**A**). ***p<0.001 compared with incubation for 0 min in control mitochondria or FCCP treated mitochondria; $^{###}$p<0.001 compared with incubation with sonicated mitochondria; §§§p<0.001 compared with incubation with FCCP treated mitochondria In (**B-E**) uptake was terminated after 2 minutes of incubation (**B-E**). In (**B**) increasing amounts of mitochondria (0.1 – 0.4 mg/ml) were used. **C**: Mitochondria (0.2 mg/ml) were

preincubated in buffer with increasing osmolarity (160 – 960 mosm/l adjusted with sucrose). ***p<0.001 compared with incubation in 320 mosm/l incubation buffer. In (**D**) uptake was started by a [^{3}H] PPX (3 µCi/ml) which was diluted with unlabeled PPX (0 - 10mM), normalized on time and taking the excess of unlabeled PPX into account. The specific rate of total PPX uptake is shown as a function of the total PPX concentration. (**E**) Uptake was measured in the presence of different energy substrates (buffer only, succinate 5 mM, ATP 1 mM or malate plus puruvate at 2.5/ 5 mM). Depolarization of mitochondrial membrane potential was induced by addition of ADP plus phosphate (both 1 mM), valinomycin (Val, 1 µM), $CaCl_2$ plus phosphate (100 nmol/mg, 1 mM), rotenone (Rot,5 µM) or FCCP (1 µM). ***p<0.001 compared with malate/pyruvate, §p<0.05, §§p<0.01, §§§p<0.001 compared with incubation in absence of energy substrates.

Figure 3: Antioxidative effects of PPX and SND, related to hydrogen peroxide.

(A) ROS were generated by xanthine oxidase in a solution containing EUK-134 (black bars), PPX (light grey bars) or SND (dark grey bars) at the indicated concentrations. To avoid competition of the compounds with the detection system, ROS-generation was stopped after 20 min by addition of allopurinol (1mM) and the non-detoxified H_2O_2 was detected by addition of AR and HRP and normalized to the amount in the absence of an antioxidant (white bar). **(B)** Mitochondrial H_2O_2 release was started by addition of mitochondria (0.1 mg/ml) to a mixture of Amplex Red 10 µM, HRP (0.4 units/ml) and succinate (2.5 mM; Ctrl) and compared to the rate of Amplex Red oxidation in the presence of PPX (300 µM) and EUK-134 (30 µM). Fluorescence of generated resorufin was detected every 30 seconds over a period of 5 minutes. After linear regression, the slopes were normalized to the control incubation and are given as mean ± SD from 3

independent experiments. **(C)** Oxidative stress was induced in HT-22 cells by Glutamate (5 mM; Glu). Cells were treated with PPX (1 mM), SND (1 mM) and EUK-134 (250 µM), with or without simultaneous addition of glutamate. After 24 hour incubation, cell viability was measured by reduction of Alamar Blue. Measurement from vehicle-treated cells is shown as a control. Data shown are mean ± SD from 8 independent experiments.

Figure 4: Antioxidative effects of PPX and SND, related to nitric oxide generated by DETA. Generation of nitric oxide was initiated by addition of DETA to a solution containing diaminofluorescein (DAF) and PPX (filled circles) or SND (open circles, both 0-10000 µM). The generation of DAF-triazole fluorescence was measured at RT every 30 s during 30 min. The obtained slopes were plotted against the concentration of PPX. The data represent mean ± SD of a representative experiment each done in triplicates.

Figure 5 : Antioxidative effect of PPX in vivo

Activity **(A)** and expression **(B)** of mitochondrial aconitase after treatment of C57BL6 mice with PPX (2 x 30 mg/kg per day, n=8) or vehicle (Ctrl, n= 6) has been determined as described in materials and methods. The data are shown as mean± SD of n animals. ***p* <0.01 by unpaired Student t-test.

Figure 6: Treatment of SOD1(G93A) transgenic mice with PPX and SND

(A) Motor activity of mice treated with vehicle (Ctrl; open circles), SND (100 mg/kg p.o.; black circles) or PPX (3 mg/kg p.o.; grey circles) was measured by recording revolutions of each running wheel in the dark period (8 p.m- 8 a.m.). Measurements were taken from day 80 to death. The resulting time performance values (insert given as mean ± SEM)

and the curve resulting from the non-linear regression are shown for each group. **(B)** Survival times are represented in a Kaplan-Meier-Plot. Statistical analysis was performed by a Logrank Mantel-Cox test using the software package SAS Version 8.2.

JPET Fast Forward. Published on September 27, 2005 as DOI: 10.1124/jpet.105.092312
This article has not been copyedited and formatted. The final version may differ from this version.

	plasma [µM]	Brain [µM]	accumulation factor brain/plasma
PPX	1.0 ± 0.2	5.4 ± 1.0	6.7 ± 1.3
SND	0.43 ± 0.09	2.5 ± 1.0	6.4 ± 1.2

Table 1 a: Plasma and brain levels of PPX and SND-treated C57BL/6 mice. Drugs were applied *per os* twice daily (7 a.m., 7 p.m.; 4 mice per group; 200 mg/kg) for 4 consecutive days. On day 5, the animals were sacrificed 12 hours after the last treatment. The data represent mean ± SEM of 4 animals. The accumulation factor was determined for each animal individually, before mean ± SEM was determined.

Per os dosage of SND [mg/kg/d]	plasma level [nM]
30	45 ± 7
100	160 ± 35
300	616.5 ± 360

Table 1 b: Plasma levels of SND-treated animals. SOD1-G93A mice were treated with SND *per os* (30, 100 and 300 mg/kg/d) from day 45 (age). At 90 days, animals were sacrificed and SND plasma levels were determined. The data represent mean ± SEM of 4 animals.

figure 1

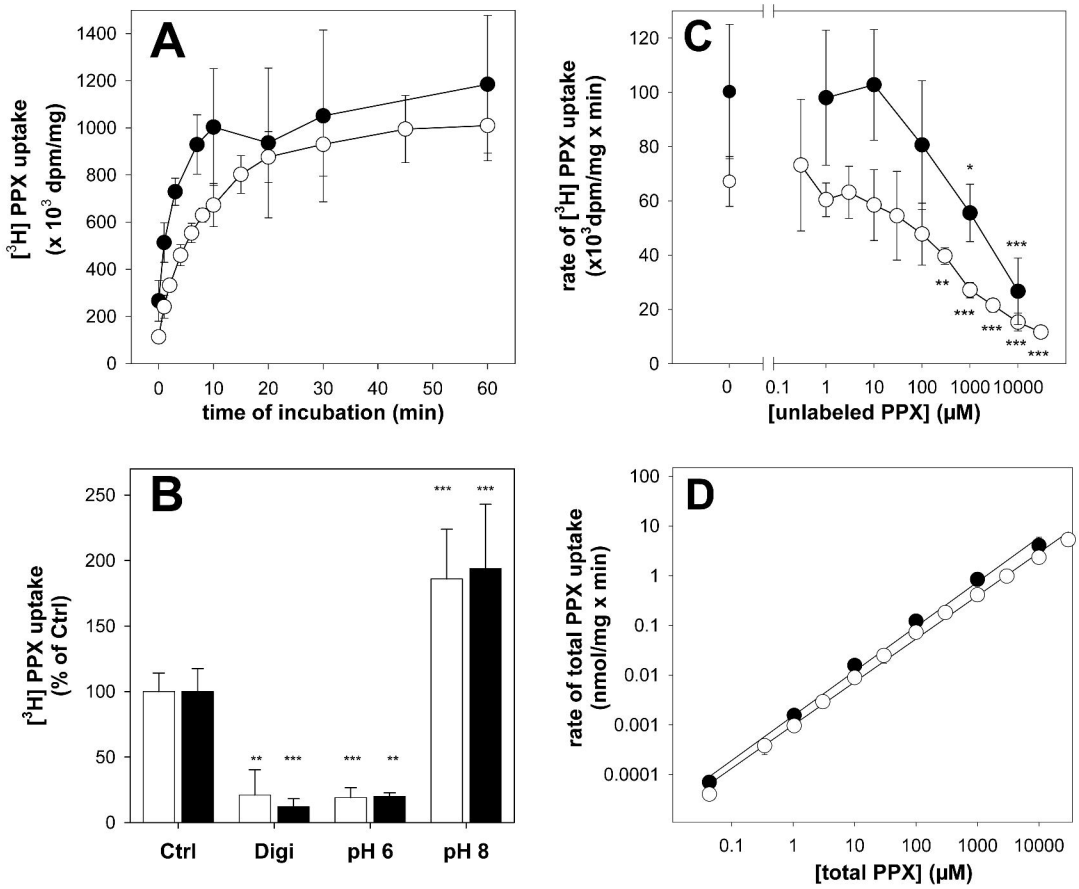
A
[3H] PPX uptake (x 10^3 dpm/mg)
time of incubation (min)
B
[3H] PPX uptake (% of Ctrl)
Ctrl
Digi
pH 6
pH 8
C
rate of [3H] PPX uptake (x10^3 dpm/mg x min)
[unlabeled PPX] (µM)
D
rate of total PPX uptake (nmol/mg x min)
[total PPX] (µM)

figure 2

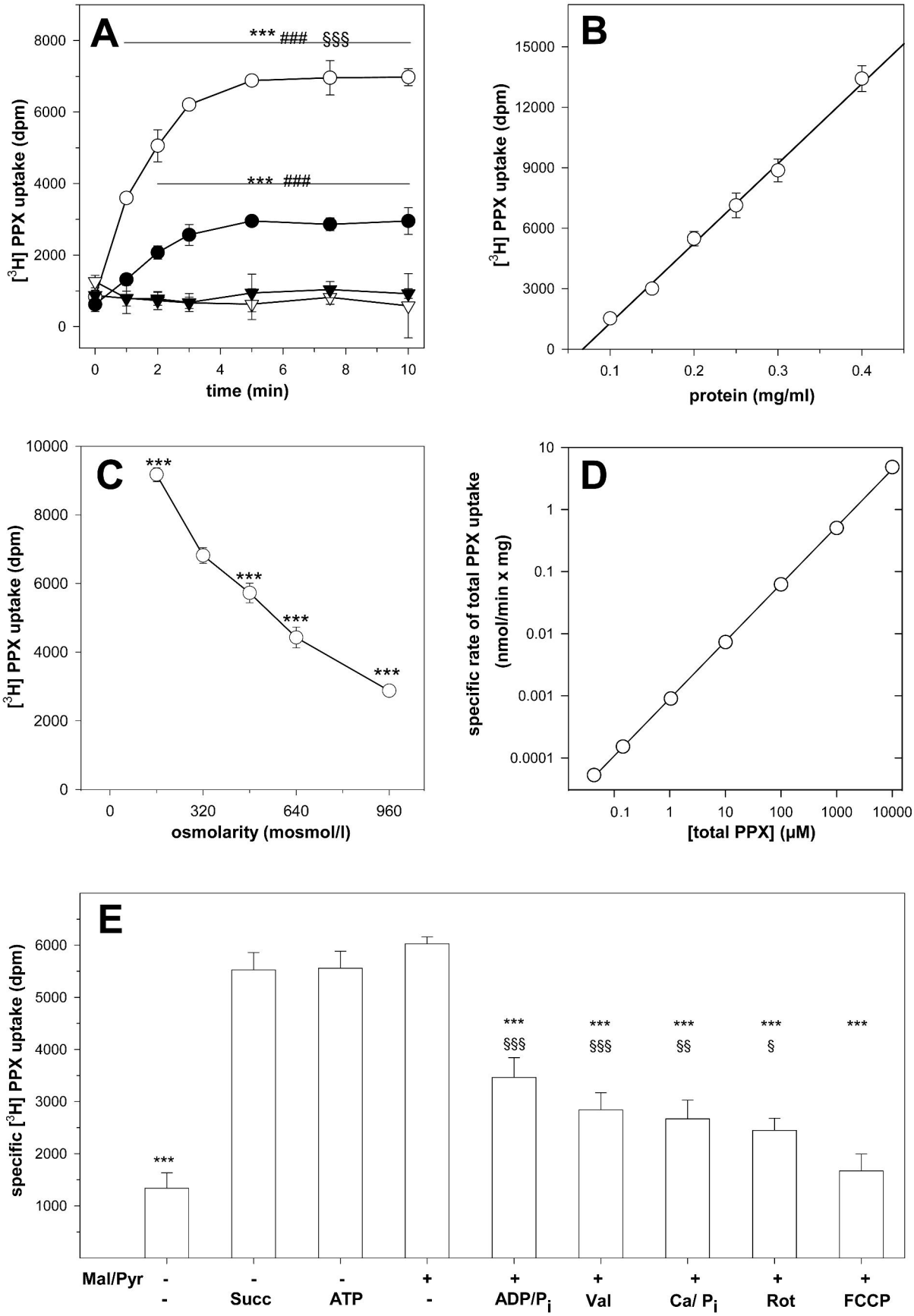

figure 3

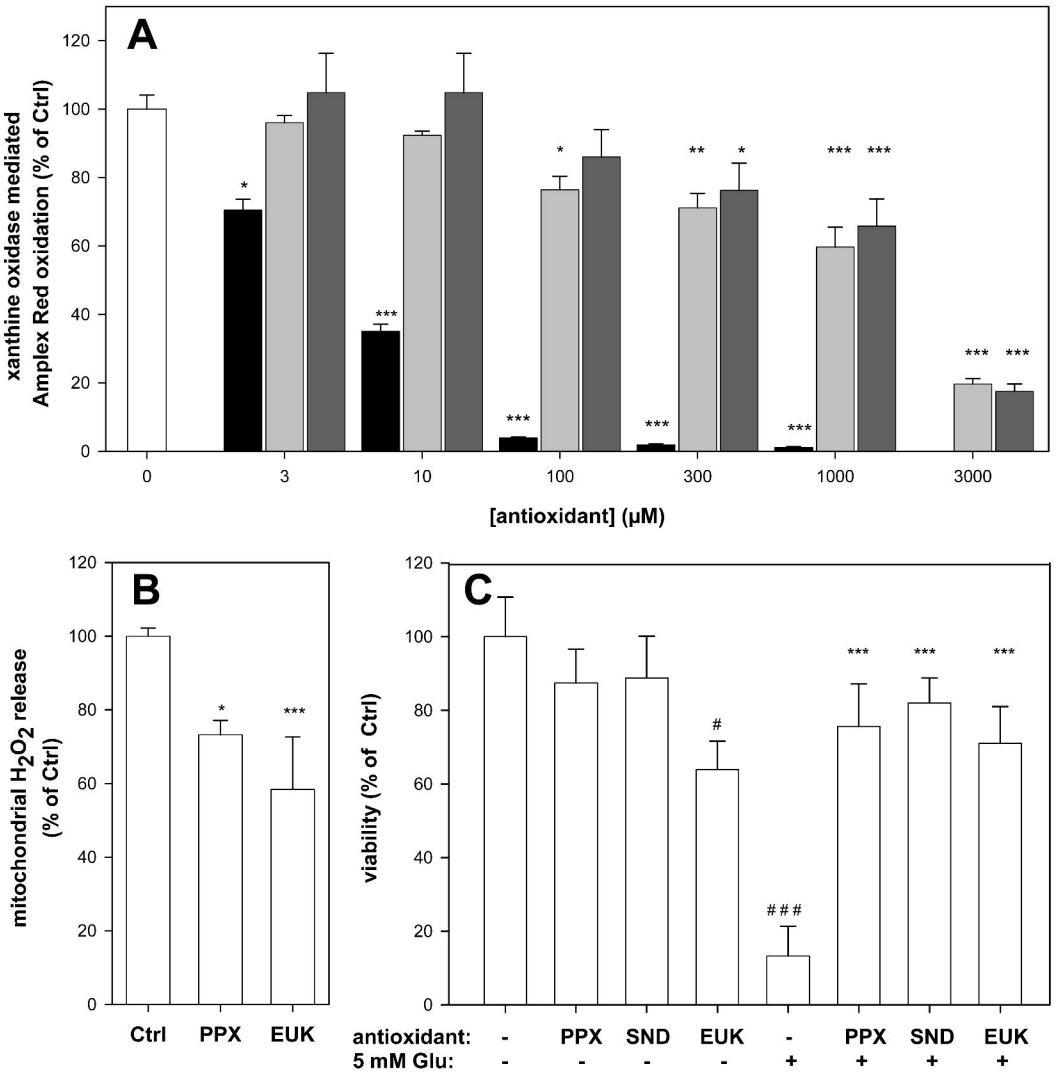

figure 4

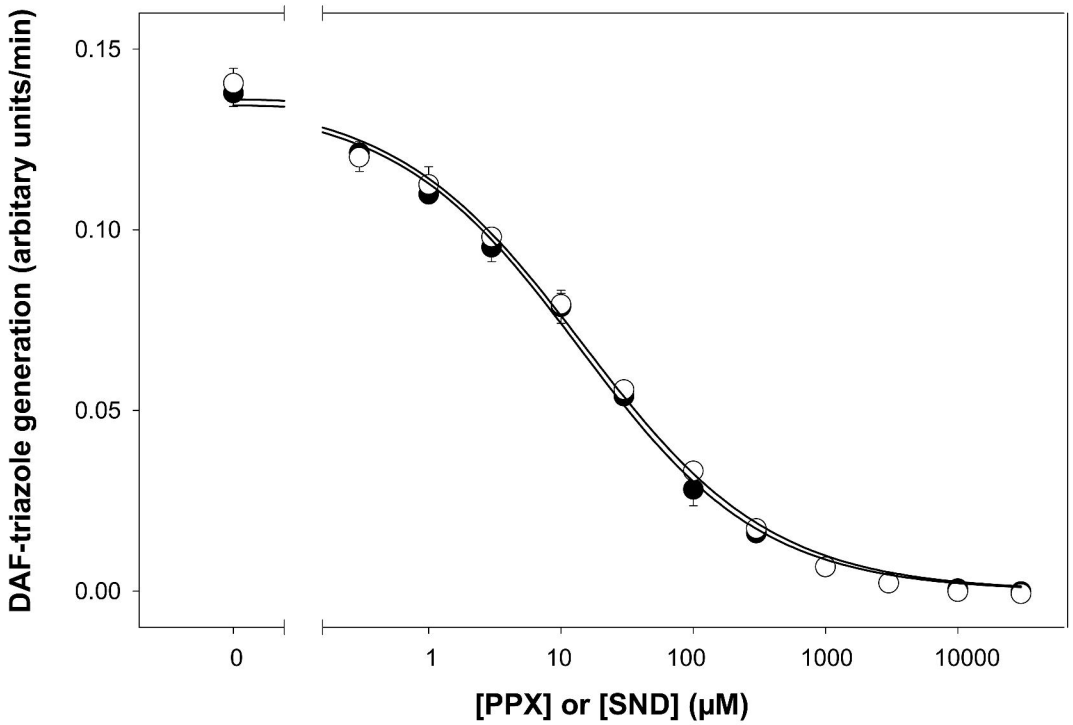

figure 5

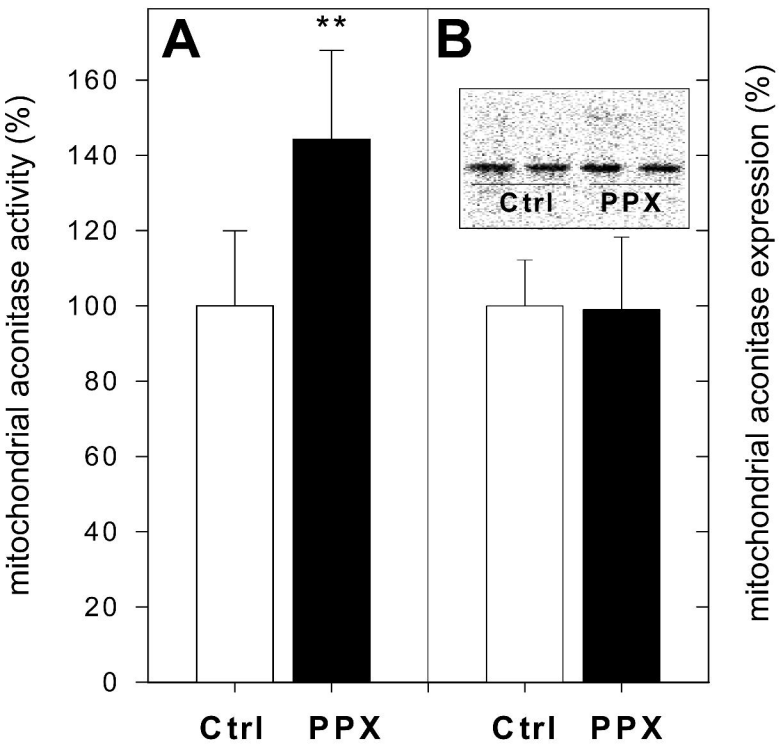

figure 6

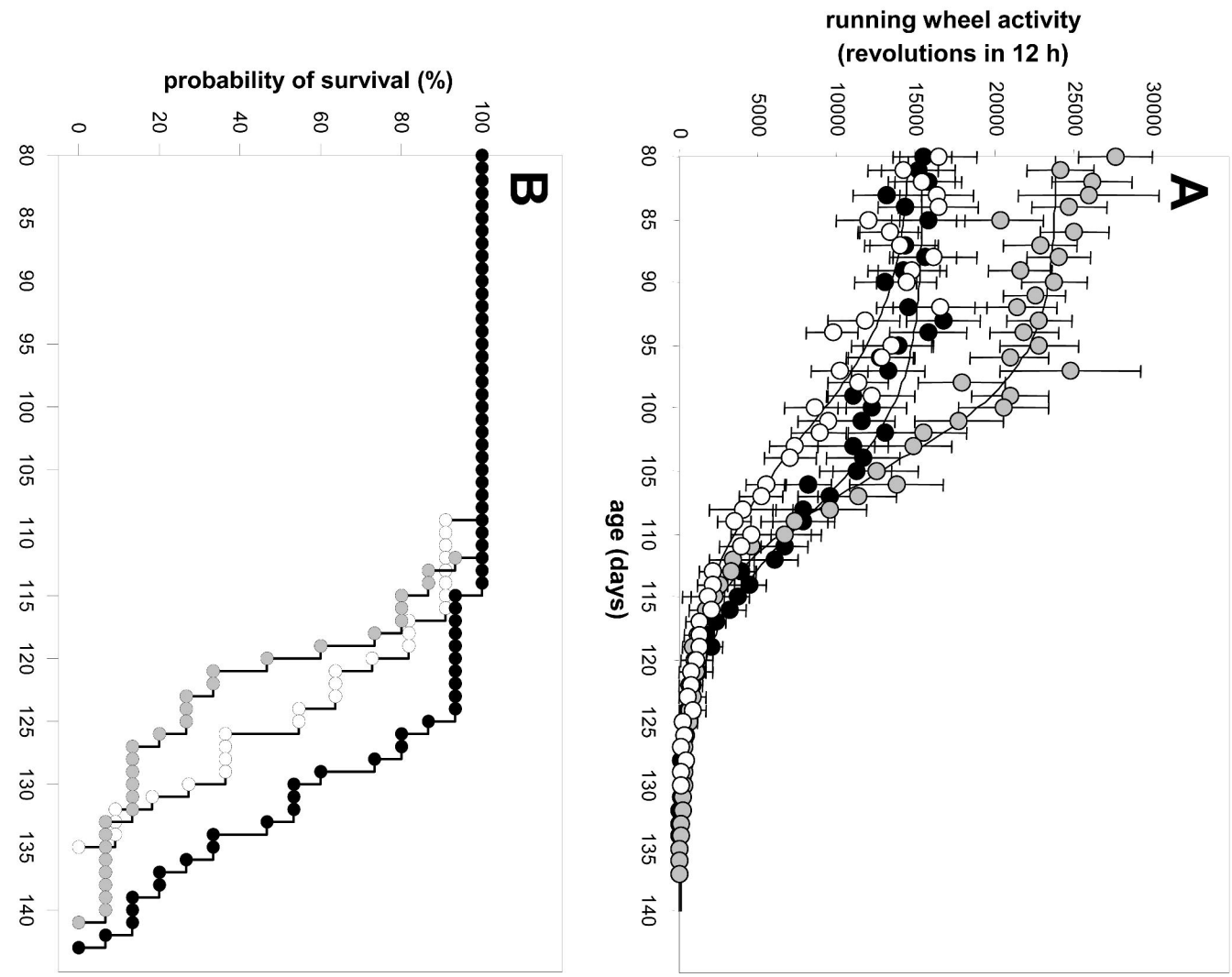
A
running wheel activity
(revolutions in 12 h)
0
5000
10000
15000
20000
25000
30000
80
85
90
95
100
105
110
115
120
125
130
135
140
age (days)
B
probability of survival (%)
0
20
40
60
80
100
80
85
90
95
100
105
110
115
120
125
130
135
140
age (days)